Prolific Polymorph Generator ROY in Its Liquid and Glass: Two Conformational Populations Mirroring the Crystalline-state Distribution

Zhenxuan Chen[1], Yue Gui[1], Kai Cui[2], J. R. Schmit[2], and Lian Yu[1]*

[1]School of Pharmacy, University of Wisconsin-Madison, Madison, Wisconsin 53705, United States

[2]Theoretical Chemistry Institute and Department of Chemistry, University of Wisconsin-Madison, Madison, Wisconsin 53706, United States

*Corresponding author: Lian Yu, Email: lian.yu@wisc.edu

Abstract

5-methyl-2-[(2-nitrophenyl)amino]-3-thiophenecarbonitrile, dubbed ROY for its numerous crystal polymorphs of red, orange, and yellow colors, has been studied in its liquid and glassy state by infrared spectroscopy. Two populations of conformers are observed whose equilibrium is characterized by ΔH = 2.4 kJ/mol and ΔS = 8.0 J/K/mol. The two populations correspond to the global and local minima of the torsional energy surface and to the conformational preference of the 13 crystal polymorphs. The local minimum features a more coplanar arrangement of the two aromatic rings, greater π conjugation, and lower CN stretch frequency. In the gas phase, the lowest-energy path between the two minima has an energy barrier 3.9 kJ/mol above the global minimum, consistent with the rapid equilibration between the two populations. The relevance of our result for understanding the prolific polymorphism of ROY is discussed.

Introduction

For over two decades, 5-methyl-2-[(2-nitrophenyl)amino]-3-thiophenecarbonitrile (Fig. 1) has been continuously studied for its large and growing number of crystal polymorphs.[1,2,3,4,5,6,7] The molecule is named ROY for its crystals of red, orange, and yellow colors and is the current record for the largest number (13) of ambient-condition polymorphs with solved crystal structures.[8] This prolific polymorphism has made ROY a model for polymorph discovery, crystal structure prediction,[9,10,11,12] and studies of structure-property relationships.[13,14,15]

ROY is noted for its conformational diversity in the crystal polymorphs. In the 13 structures, ROY adopts a wide range of conformations characterized by the torsional angles defined in Fig. 1. For example, θ_{thio} ranges from 5° (in polymorph R18)[6] to 128° (polymorph PO13).[5] This variation explains the different crystal colors:[13] small θ_{thio} means that the two aromatic rings are nearly coplanar, which promotes π conjugation and leads to a deeper color (red); as θ_{thio} increases, the extent of π conjugation decreases and the crystal color changes to orange and yellow. Recently, Tang et al. observed that inclusion of ROY in hydrogen-bonded frameworks tends to flatten the molecule.[16]

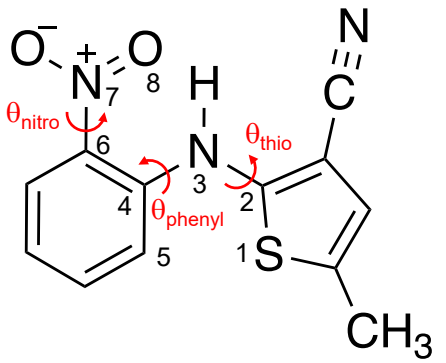

Fig. 1. Molecular structure of ROY. Definition of torsional angles: $S_1C_2N_3C_4$ (θ_{thio}), $C_2N_3C_4C_5$ (θ_{phenyl}), $C_4C_6N_7O_8$ (θ_{nitro}).

Given its conformational diversity in the crystalline state, it is of interest to determine ROY's conformation in the liquid state. Does the distribution of conformers in crystals have a counterpart in the liquid phase? Does the liquid-state conformation influence the crystallization process and polymorphic selection? In this work, infrared (IR) spectroscopy and quantum chemical calculations are used to investigate the conformational distribution of ROY in its liquid and glass. We find that ROY exists in two conformational populations whose equilibrium is characterized by ΔH = 2.4 kJ/mol and ΔS = 8.0 J/K/mol. These two populations correspond to the global and local minima of the torsional energy surface and to two groupings of conformers observed in the crystal polymorphs. Our result confirms the importance of intramolecular energetics in the formation of crystals and in crystal structure prediction.

Experimental

ROY was a gift from Eli Lilly and Company. IR absorption spectra were recorded in transmission with a Bruker Equinox 55/S FT–IR unit or a Nicolet 60SXB spectrometer. The instruments had a resolution of 4 cm^{-1}, consistent with the full width at half maximum (FWHM) of the peaks of the ROY crystal spectra. To measure the liquid-phase spectrum, a crystalline powder was melted between two KBr disks and the resulting liquid film was mounted on a custom-built temperature stage. The temperature of the stage was controlled between 250 and 365 K by circulating cooled ethanol or heated water through a brass block using a VWR PolyScience circulator. The block temperature was calibrated against the melting point of *o*-terphenyl crystals (329 K). To measure the solution spectra, a ROY powder was dissolved in chloroform or carbon tetrachloride at target concentrations and IR absorption spectra were recorded at 295 K.

The gas-phase geometry of ROY was optimized by the Møller–Plesset perturbation theory (MP2) with the cc-pVDZ basis set using Gaussian16.[17] The initial structure was the molecule in the crystal structure of ROY polymorph ON (QAXMEH in the Cambridge Structural Database).[1] Geometry optimization was performed either without constraints, yielding the global and local minima, or at fixed θ_{thio} (Fig. 1), yielding the torsional energy vs. θ_{thio} curve. The transition states for conformational changes were searched using Nudged Elastic Band (NEB) theory implemented in the Atomic Simulation Environment (ASE).[18,19] For each search, the initial and the final conformations were provided and the transition state was sought that had only one imaginary frequency corresponding to the saddle point on the reaction path between the two structures. The search was also performed at the level MP2/cc-pVDZ.

Results and Discussion

IR Spectroscopy

In this work, the CN stretch band in the IR spectrum was used to study the molecular conformation of ROY. The CN stretch occurs in an uncrowded region of spectrum, enabling detailed analysis of its position, width, and shape without interference from other vibrations. It has been used to study the local environment of proteins[20,21] and solvents.[22,23] For ROY, the CN stretch frequency is sensitive to the molecular conformation as seen from a comparison of the crystal polymorphs in which ROY adopts different conformations (see below).[1]

Fig. 2a shows the typical spectrum of a ROY liquid as a function of temperature. Each spectrum contains a main peak and a shoulder at lower wavenumber. With cooling from 360 K to 250 K, the main peak rises and the shoulder decreases, as indicated by the arrows. The regions of increase and decrease are separated by an isosbestic point at 2222 cm^{-1}, at which the absorbance is invariant. As we discuss below, the isosbestic point is indicative of two conformational populations in equilibrium with each other. The gap in the progression of spectra is a result of skipping a temperature range at which crystallization was fast. As we see later, this had no consequence in determining the temperature dependence of the spectrum.

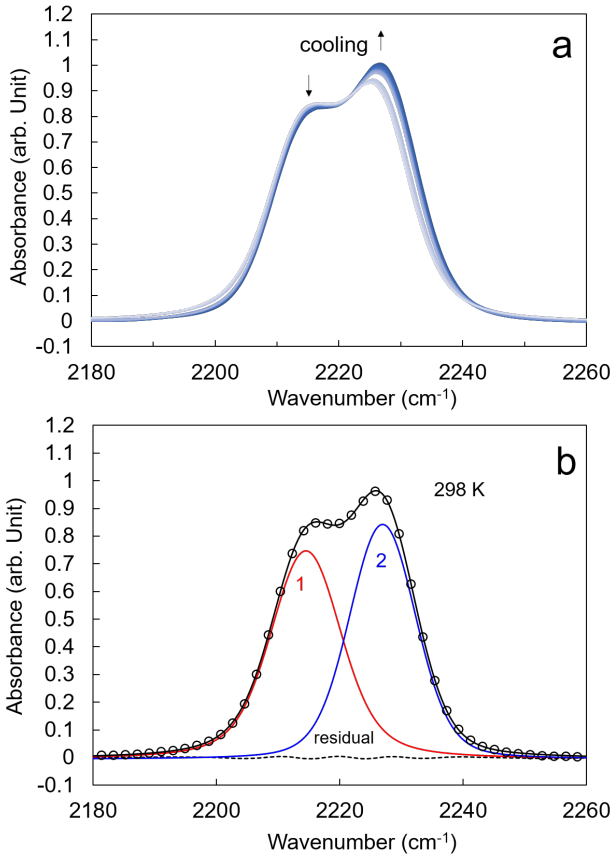

Fig. 2. (a) CN stretch spectra of ROY melt from 250 K to 360 K. The gap in the progression of spectra was a result of skipping a temperature range in which crystallization was fast. (b) Illustration of the fit of each experimental spectrum (this one recorded at 298 K) using two Voigt functions.

We find that each spectrum observed is well fitted as a sum of two Voigt functions. Fig. 2b illustrates this fit where 1 and 2 refer to the peaks at lower and higher wavenumbers,

respectively. The small residual displayed at the bottom indicates the quality of fitting. This fit yields the position, the width, and the area of each peak. These fitting parameters are plotted in Fig. 3 as a function of temperature.

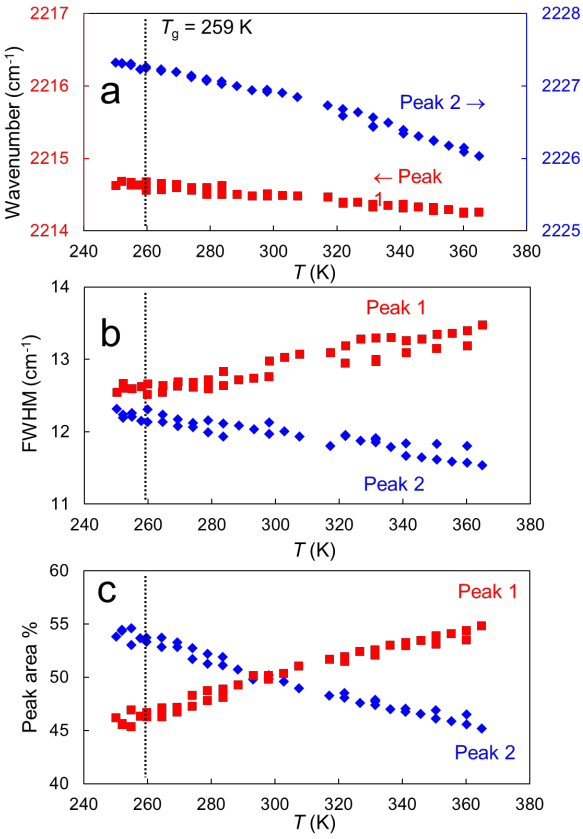

Fig. 3. The temperature dependence of (a) peak position, (b) peak width (FWHM), and (c) relative peak area for each of the two peaks that compose the observed CN stretch band (Fig. 2b).

Fig. 3a shows that with cooling, both peaks shift to higher wavenumbers (blue shift), with Peak 2 showing larger shift. As a result, the separation between the two peaks increases with cooling. Fig. 3b shows the FWHM of each peak as a function of temperature. Peak 1 is slightly broader than Peak 2, and with cooling, Peak 1 narrows while Peak 2 broadens. We note that these peak widths have contributions from the instrumental resolution (4 cm^{-1}) but their differences and temperature trends are considered reliable. Fig. 3c compares the areas of the two peaks, each expressed as a percentage of the total area. With cooling, the area of Peak 2 increases at the expense of Peak 1 and the two areas are the same at 295 K. The vertical dotted line in Fig. 3 indicates the glass transition temperature of ROY, T_g = 259 K. Within the temperature range investigated, none of the spectral characteristics considered above is sensitive to the passage of T_g.

We interpret the results above as follows. Peaks 1 and 2 correspond to two populations of ROY conformers in equilibrium with each other. This conclusion is supported by the success of the two-peak model to fit each spectrum (Fig. 2b) and by the observation of the isosbestic point at 2222 cm^{-1} (Fig. 2a). At the isosbestic point, the two conformers have the same extinction coefficient so that any change of their concentrations does not alter the sum of the total absorbance. The isosbestic point is a general feature of processes where the observed spectrum is the sum of the

contributions from two species that exist in equilibrium.[24,25] Given that Peak 2 increases with cooling at the expense of Peak 1, the corresponding conformation has lower energy. As we discuss later, this conformation is associated with the global minimum of the torsional energy surface.

Building on the understanding above, we calculate the equilibrium constant for the conformational change:

Low-energy conformer (Peak 2) ↔ High-energy conformer (Peak 1).

The equilibrium constant is given by

$$K = x_1/x_2 = A_1/A_2$$

where x_1 and x_2 are the mole fractions of the high-energy and low-energy conformers, with $x_1 + x_2 = 1$, and the second equality assumes that the area of each peak is proportional to the fraction of the corresponding conformer (that is, the two conformers are assumed to have the same average extinction coefficient).

Fig. 4 shows the van't Hoff plot of the equilibrium constant K (ln K vs. $1/T$). A linear relation is observed. From the linear fit, we obtain: ΔH = 2.4 kJ/mol, ΔS = 8.0 J/K/mol, where ΔH and ΔS are the enthalpy and entropy changes associated with the conformational equilibrium. The adherence of K to van't Hoff's law is further support for the two-population model for ROY conformers. It is noteworthy that the high-energy conformer (Peak 1) has approximately equal concentration as the low-energy conformer (Peak 2), with $K \approx 1$. Within van't Hoff's model, this is interpreted as a compensation effect where the high-energy conformer is disfavored in terms of enthalpy but favored in terms of entropy. The temperature range in Fig.

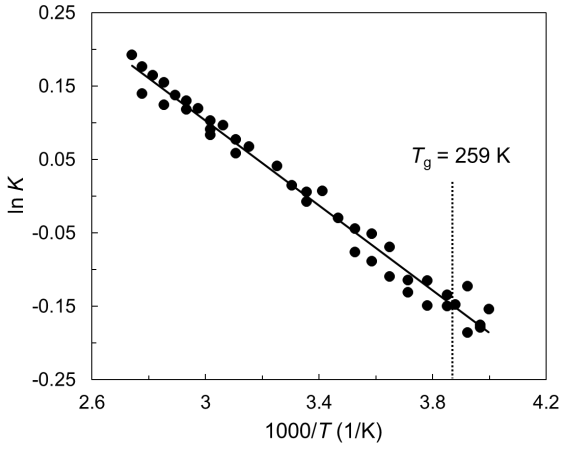

Fig. 4. van't Hoff plot of the equilibrium constant K for conformational change. From the linear fit (solid line) we obtain ΔH = 2.4 kJ/mol and ΔS = 8.0 J/K/mol.

4 spans ROY's T_g (259 K) and there is no evidence that the conformational equilibrium is perturbed by the passage of T_g. When a liquid is cooled below its T_g, whole-molecule rotation and translation are frozen, causing a drop of heat capacity. Our result thus indicates that ROY's conformational dynamics is not strongly coupled to those degrees of freedom that are frozen by the glass transition.

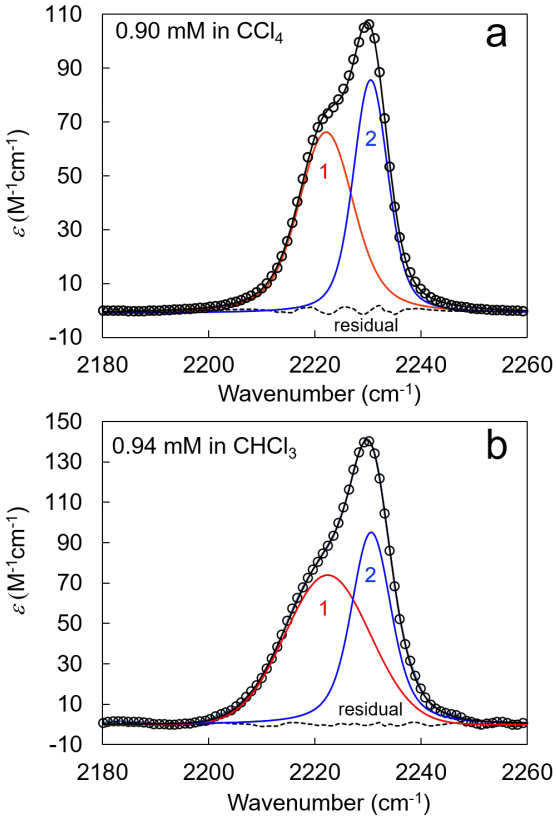

Fig. 5. CN stretch spectrum of ROY in (a) CCl_4 and (b) $CHCl_3$ at a similar concentration (~0.9 mM). Each spectrum is fitted as a sum of two Voigt functions.

The two-population model not only describes ROY conformations in the pure liquid but also in the solutions. Fig. 5 shows the CN stretch spectra of ROY dissolved in CCl_4 and $CHCl_3$ at similar concentrations (~0.9 mM). In each solution, the ROY spectrum features a main peak and a shoulder at lower wavenumber. As in the case of the melt spectrum (Fig. 2b), the solution spectrum is well represented as a sum of two Voigt functions. The two-peak fitting is illustrated in Fig. 5. The small residual shown at the bottom indicates the quality of fitting. The fitting results are collected in Table 1.

Table 1. Peak positions ν, peak area A, and peak width (FWHM) of the two components in the CN stretch spectrum of ROY at 295 K.

solvent		ν (cm^{-1})	A (%)	FWHM (cm^{-1})[a]
CCl_4	peak 1	2222	56	12
0.090 mM	peak 2	2230	44	8
$CHCl_3$	peak 1	2222	59	19
0.094 mM	peak 2	2231	41	10

None	peak 1	2214	50	13
(neat liquid)	peak 2	2227	50	12

[a] The FWHM contains the unremoved contribution from instrumental contribution (4 cm^{-1}), but their differences are considered meaningful.

Relative to the melt spectra, the solution spectra for the two solvents used are blue-shifted and the separation between the two peaks is reduced. The A_1/A_2 ratio is slightly larger in these solutions than in the melt when compared at the same temperature (295 K), indicating a larger fraction of the high-energy conformer in the solutions. The effect of changing the solvent from CCl_4 to $CHCl_3$ on the CN spectrum is the most noticeable in the peak shape: in $CHCl_3$, Peak 1 has lower height than in CCl_4. Besides this, the solvent effects on spectral features are relatively minor. For benzonitrile, Bagchi et al. observed that the CN stretch frequency is lower in solvents of higher polarity and dielectric constant and attributed the effect to increased local electric field and the vibrational Stark effect.[23] Their work could be a basis for understanding the ROY results. ROY has larger dielectric constant (50.4)[26] than CCl_4 (2.2) and $CHCl_3$ (4.8) and presumably higher local electric field and larger Stark shift. In this work, our focus is on the main result that in both the melt and the solutions, ROY exists as two populations of conformers. We seek an understanding of this result on the basis of quantum chemical calculations described below.

Quantum Chemical Calculations

The experimental finding that ROY exists in two conformational populations in its melt and solutions motivates an analysis of the torsional energy landscape. We inquire whether the landscape contains multiple minima that correspond to the observed populations and if so, how high the activation barriers are between them. The first quantum chemical calculation on ROY was performed at the level of RHF/6-31G* and observed only a single energy minimum for $\theta_{thio} > 0$ (an equivalent, inversion-related minimum occurs at $\theta_{thio} < 0$). Later work employed other computational models and reached rather different conclusions:[27, 28, 29, 30, 10, 11,] for $\theta_{thio} \geq 0$, some reported two minima, others three; when two were reported, the global minimum was placed at higher or lower θ_{thio} than the local minimum. Thomas and Spackman pointed out that many DFT methods are problematic for a molecule like ROY for they overweigh the stabilizing effect of π conjugation; they regarded MP2 energies as more accurate.[29] More recently, Greenwell et al. used

CCSD(T) as the benchmark for accurate torsional energies.[11] In this work, we revisit this problem using MP2/cc-pVDZ and investigate not only the energy minima but also the transition barriers.

Fig. 6 shows the torsional energy of ROY as a function of θ_{thio}. The energy profile shows four symmetry-related minima marked with red crosses: G+, G-, L+, and L-, where G and L indicate global and local minima and + and – distinguish degenerate inversion-related pairs. These minima were obtained by full optimization (no constraints). The results are shown in Table 2 and the inset of Fig. 6. The global minima, G+ and G-, are characterized by $\theta_{thio} = \pm 116.9°$ and the local minima, L+ and L-, by $\theta_{thio} = \pm 46.5°$. The local minima are 1.4 kJ/mol higher in energy than the global. In Fig. 6, M1, M2, and M3 indicate the maxima observed by the θ_{thio} scan. These maxima all come as inversion-related pairs distinguished by plus and minus signs. As we discuss below, these are not the transition-state points. Our results are consistent with the benchmark CCSD(T) result.[11]

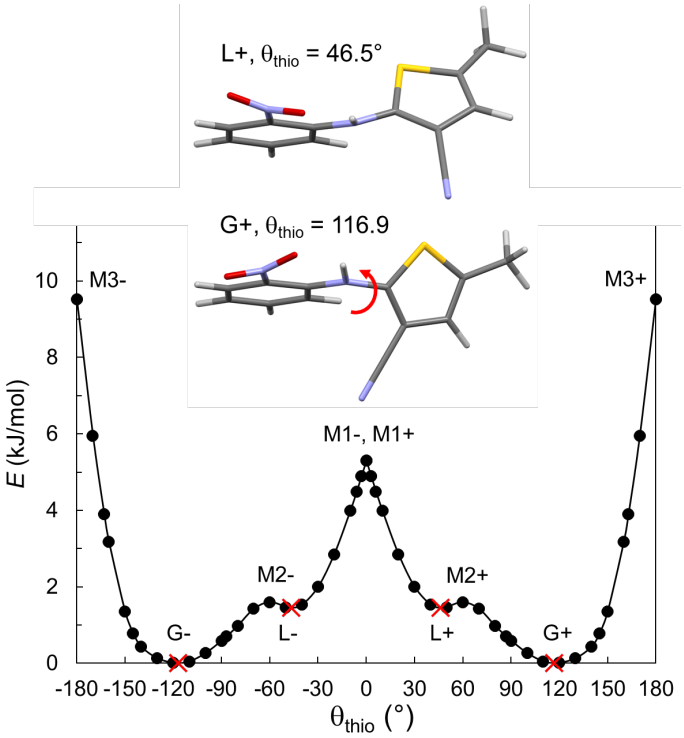

Fig. 6. Torsional energy of ROY as a function of θ_{thio} calculated using MP2/cc-pVDZ. G+, G-, L+ and L- are 4 symmetry-related global and local energy minima (marked with red crosses). The structures of G+ and L+ are shown on top. M1, M2, and M3 are the maxima of the energy profile for which + and – indicate inversion-related pairs.

Table 2. Parameters for the torsional energy surface of ROY.

State points [a]	θ_{thio} $S_1C_2N_3C_4$ (°)	θ_{phen} $C_2N_3C_4C_9$ (°)	θ_{nitro} $O_7N_6C_5C_4$ (°)	$E - E$ (global) (kJ/mol)
Minima				
G+	116.9	-0.9	16.0	0
L+	46.5	26.0	-15.5	1.4
Maxima of energy scan along θ_{thio}				
M1+	0 (fixed)	46.0	-22.0	5.3
M2+	60 (fixed)	26.8	-8.9	1.6
M3+	180 (fixed)	-61.6	24.4	9.5
Transition states				
TS1 (between L- and L+)	0.0	0.0	0.0	12.9
TS2+ (between L+ and G+)	82.4	11.9	1.2	3.9
TS3 (between G- and G+)[b]	180.0	0.0	0.0	34.4

[a] The plus sign (+) indicates one of two inversion-related iso-energy structures. For the other structure in each pair (with the minus sign (-)), reverse the signs of all torsional angles. Where no plus or minus sign is given (TS1 and TS3), the structure is planar and achiral.

[b] The actual TS search yielded a slightly non-planar structure with θ_{thio} = 179.1°, θ_{phen} = 1.5°, and θ_{nitro} = 2.6°, but we regard the deviation from planarity as insignificant.

The global and local energy minima obtained by quantum chemical calculations correspond reasonably well with the conformational preference of ROY in the crystalline state. In Fig. 7, a histogram is shown of the θ_{thio} angle for the 13 polymorphs of ROY[1,2,3,4,5,6,7,8] and 6 guanidinium organosulfonate (GS) inclusion compounds containing ROY.[16] ROY adopts a wide range of conformations in the crystalline state with θ_{thio} ranging from 5° to 128°. The polymorphs (black

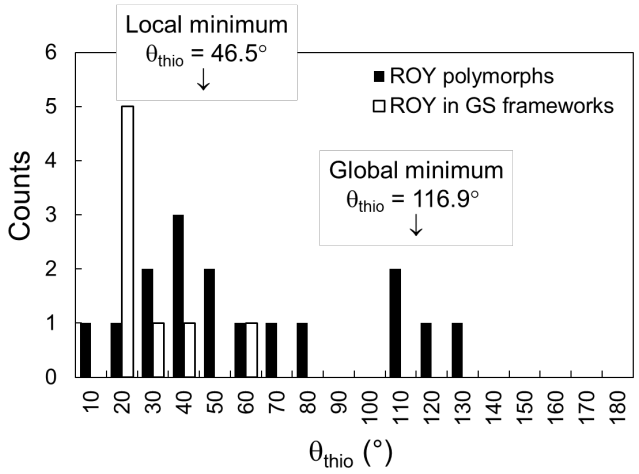

Fig. 7. Histogram of θ_{thio} for ROY in its 13 polymorphs and 6 guanidinium organosulfonate (GS) inclusion compounds. Some structures contain independent molecules, making the total count greater than 13 (for polymorphs) or 6 (for inclusion compounds).

bars) fall into two groups, one centered around 40° and the other around 110°. These two groups approximately correspond to the local and the global minima, indicated by down arrows. This indicates that the conformational preference in the crystalline state has correspondence with that in the gas phase. It is also noteworthy that more crystal structures are clustered around the local minimum than around the global minimum. That is, despite its higher energy, the local-minimum conformer (with some adjustment) is utilized more often as the building block in the observed crystal structures. On the other hand, the global-minimum conformer (with some adjustment) is the building block for the two lowest-energy polymorphs: Y with θ_{thio} = 104.7° and YT04 with θ_{thio} = 112.8°. In the GS frameworks, ROY conformations are clustered exclusively around the local minimum. These rich observations reflect an interplay between the intrinsic conformational bias and the preferred conformation for crystal packing.

The torsional energy curve of ROY in Fig. 6, valid for a gas-phase molecule, also provides a basis for understanding its two conformational populations in the liquid state. Assuming the liquid environment does not significantly alter the conformational preference, we expect two populations of conformers whose structures fall close to the global and local minima. These two populations are expected to have different CN stretch frequencies, with the higher frequency associated with the global-minimum conformer. This last expectation is based on the fact that in ROY polymorphs[1,2,3,4,5,6,7,8] and inclusion compounds,[16] higher CN stretch frequency correlates with larger θ_{thio}. This correlation is displayed in Fig. 8. In addition to ROY, Fig. 8 includes two data points on the polymorphs of "nor-methyl ROY" (ROY without its methyl group).[31] This correlation arises because smaller θ_{thio} leads to a more co-planar structure, enabling stronger π electrons conjugation between the two aromatic rings and causing a decrease of the CN stretch frequency. Based on this explanation,

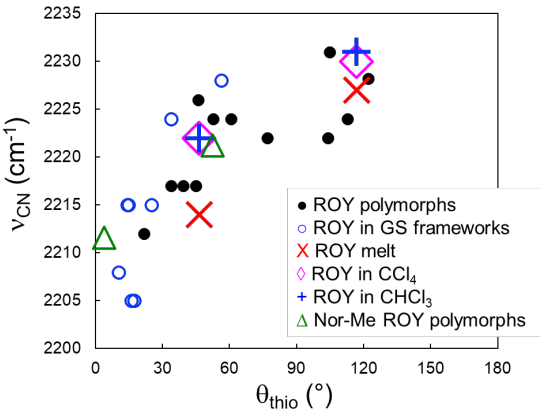

Fig. 8. CN stretch frequencies of ROY polymorphs and inclusion compounds plotted against θ_{thio}. The data points for ROY melt and solutions are placed at θ_{thio} = 46.5° (local minimum) and 116.9° (global minimum). In addition, we include the data points on the two polymorphs of ROY with its methyl group removed (nor-Me ROY).

lower temperature favors the global-minimum conformer (Peak 2). This is in complete agreement with experiment: with cooling, Peak 2 increases at the expense of Peak 1 (local minimum). The 1.4 kJ/mol energy difference between the global and the local minima is close to the 2.4 kJ/mol enthalpy difference between the two groups of liquid-state conformers. The difference can arise from many factors, including zero-point energy and solvation effect.

We now turn to the transition states (TS) and the energy barriers for conformational changes. This information is important for understanding the rate of transitions. Given that our experiments observed no out-of-equilibrium behavior during heating or cooling, the timescale for conformational changes must be short relative to the experimental timescale – minutes to hours, implying relatively fast transitions and low energy barriers. Naïvely, the TS points are simply the maxima of the energy scan in Fig. 6 (M1, M2, and M3). But this is not the case, as our TS searches found energy barriers significantly higher than these maxima (Table 2). In each search, we begin with two input structures (the initial and the final conformations) and seek a saddle point where the energy is minimal with respect to all vibrations except for one – the reaction coordinate. With L+ and L- as input, a TS is located at θ_{thio} = 0° (TS1), 11.5 kJ/mol higher in energy than the input structures. As shown in Fig. 9, this is a planar, achiral structure, expected for a transition state between two chiral structures of opposite sense (L+ and L-). With L+ and G+ as input, we obtain a TS at θ_{thio} = 82° (TS2+) whose energy is 3.9 kJ/mol above G+ and 2.5 kJ/mol above L+. This is a non-planar, chiral structure for the transition between two structures of the same chirality (G+ and L+). (By symmetry, there is an inversion-related transition state TS2- for the transition between G- and L-.) Finally, with G+ and G- as input, a TS at θ_{thio} = 180° (TS3) is located whose energy is 34.4 kJ/mol higher than the input

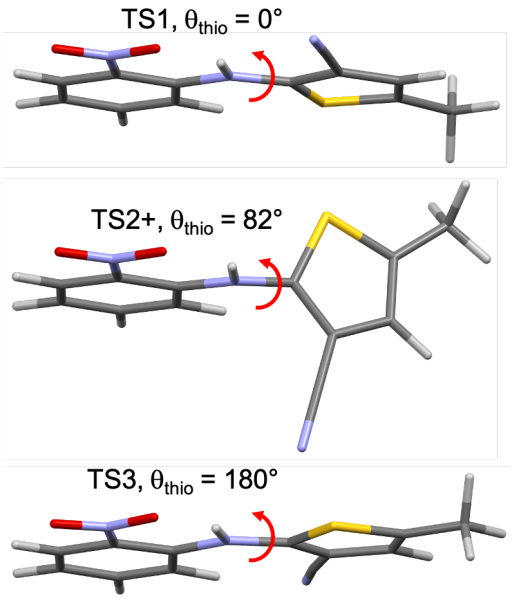

Fig. 9. Structures of the transition states for conformational changes. TS1 is for the transition between the two local minima L+ and L-. TS2 is for the transition between the global and local minima of the same chirality with chirality distinguished by + and – signs. TS3 is for the transition between the two global minima G+ and G-.

structures. As in the case of TS1, TS3 is a planar, achiral structure, as expected for the transition between two chiral structures (G+ and G-).

The set of energy barriers obtained by the transition-state search is insufficient to cause kinetic arrest in the temperature range investigated. The height of TS2 is on the order of thermal energy *kT* relative to the states connected by it (G+ and L+ or G- and L-). This is consistent with the lack of any out-of-equilibrium behavior observed in this work (Fig. 3 and 4). It is also important to note that the energy barriers above pertain to isolated molecules in the gas phase and are likely modified by the condensed-phase environment. For example, the energy of TS1 is a sizable 12.9 kJ/mol above the global minimum, but a known polymorph of ROY (R18)[6] actually utilizes a nearly identical conformer as TS1 as building unit. In this case, the conformational strain is apparently overcome by the stabilizing effect of crystal construction. Given the high dipole moment of the planar TS1 structure,[1] one mode of stabilization is the dipole-dipole interaction. The stabilization of TS1 in this manner would accelerate the conformational transition between L+ and L-. Of the three TS points identified, TS3 has the highest energy (34.4 kJ/mol above the global minimum), suggesting the conversion between G+ and G- is the slowest and could be frozen at low enough temperatures.

Given the common use of 1D torsional scans of the type in Fig. 6, we briefly discuss the failure of this method to identify the transition states for conformational changes. As Table 2 shows, the TS points are significantly higher than the maxima of the 1D scan at the same θ_{thio}. The discrepancies are 7.6 kJ/mol for TS1, 2.3 kJ/mol for TS2, and 24.9 kJ/mol for TS3. This failure is an intrinsic issue for a molecule like ROY with many coupled torsions (Fig. 1).[32] The torsional energy of ROY is a function of all its major torsional angles (θ_{thio}, θ_{phen}, and θ_{nitro}).[33] In the 1D scan, slices are taken of the multi-dimensional potential energy surface, each at a fixed θ_{thio}, to find the minimum on each slice. At fine enough increments, a 1D slice is guaranteed to cut through a TS saddle point, but depending on the topology of the energy surface, the TS point is not guaranteed to be a minimum on the slice and as a result, may be absent in the search report.[32] We illustrate this in Fig. 10 where ROY's torsional angles θ_{phen} and θ_{nitro} are plotted as θ_{thio} is scanned between the local minima L- and L+. The TS point between L- and L+ is located at the center of each plot, corresponding to a planar structure with $\theta_{thio} = \theta_{phen} = \theta_{nitro} = 0°$. Note that during the θ_{thio} scan,

the system's trajectories do not pass through the TS point. At $\theta_{thio} = 0$, the θ_{thio} scan yields two structures, M1+ and M1-, depending on the direction of approach; these structures have the same energy but opposite chirality. The dotted lines indicate the hypothetical reaction path between the two minima through the TS. The above discussion explains the unusual "pointy" maxima M1 and M3 of the torsional energy curve in Fig. 6. The pointy maxima imply a discontinuity in the first derivative of energy and a singularity in the second derivative, features incompatible with a real potential energy surface. This "anomaly" is a result of projecting trajectories on a multi-dimensional surface onto one dimension. For example, in Fig. 10, M1+ and M1- are two distinct structures, but they coincide when projected unto one dimension (θ_{thio}) because both are characterized by $\theta_{thio} = 0$. In Fig. 6, changing θ_{thio} from slightly below zero (M1-) to slightly above (M1+) is not a continuous path, but a jump on the multi-dimensional energy surface (Fig. 10), leading to the pointy maximum. Although the maximum M2 appears less pointy than M1 and M3, the same underlying issue[32] likely exists. For this reason, TS2 is to be trusted over M2 as representing the barrier for conformational transitions. As future work, a grid scan near M2 would be informative to determine the reaction path.

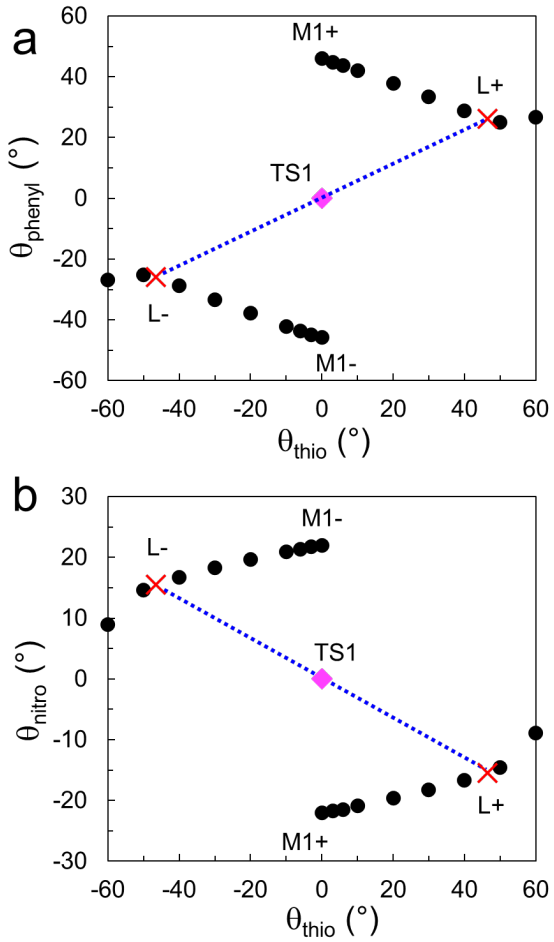

Fig. 10. Changes of ROY torsional angles θ_{phenyl} (a) and θ_{nitro} (b) during a 1D energy scan along θ_{thio}. Only the region around $\theta_{thio} = 0$ is shown. The diamond symbol at the center indicates the transition state TS1.

Concluding Remarks

In this work, the IR spectrum of ROY is used to investigate its conformations in the melt and in solutions. In both media, ROY exists as two populations that correspond to the global and the local minima of the torsional energy surface. The global minimum corresponds to a more orthogonal

arrangement of the two aromatic rings, with reduced π conjugation and higher CN stretch frequency. The equilibrium between the two populations in the melt is characterized by ΔH = 2.4 kJ/mol and ΔS = 8.0 J/K/mol. The lowest-energy pathway connecting the global and the local minima has a transition state 3.9 kJ/mol above the global minimum, allowing rapid equilibration between the two populations.

The temperature range of our measurement extends from well above the glass transition temperature (T_g = 259 K) to 10 K below and we observed no evidence that the conformational equilibrium is perturbed by the passage of T_g. At the glass transition, whole-molecule rotation and translation are frozen, causing a drop of heat capacity. Our result indicates that the conformational dynamics of ROY is decoupled from those degrees of freedom that are frozen by the glass transition. It would be of interest to investigate the system at lower temperatures to observe the kinetic arrest of conformational dynamics.

The low barrier of conversion between ROY conformers suggests the possibility to observe spectral coalescence and splitting as a function of temperature, as commonly investigated by dynamic NMR.[34] The high frequency of the CN stretch implies that to observe this effect, the exchange rate would need to be extremely fast, on the order of THz. There have been some examples of spectral coalescence in the IR regime; for example, the CO stretch bands of (η^4-norbornadiene) $Fe(CO)_3$ merge with heating[35] and the CN stretch band of acetonitrile in methanol is split into free and hydrogen-bonded components but unresolved at high temperatures.[36] Our data show only a weak hint of coalescence – see the decrease of peak separation with heating in Fig. 3a, and the temperature effect is far smaller than in the two examples given above. It might be possible to use dynamic NMR to study the ring rotation and inversion dynamics in ROY.[37,38] The transition barriers at θ_{thio} = 0 and 180° (TS1 and TS3, Fig. 9) are comparable to those that have been investigated by dynamic NMR.[39,40]

There have been attempts to connect liquid-state conformation with crystallization and polymorphic selection, hypothesizing that conformational similarity between the liquid state and a crystal structure promote crystallization toward that structure.[41,42] In the case of ROY, there is some validity in this statement in that the two populations of conformers in the liquid state

approximately match the two populations in the crystalline state (Fig. 7). This argues that conformational preference in the liquid state is not lost when forming crystals. It is consistent with the finding that accurate conformational energies are important in the energy ranking of crystal polymorphs.[10,11] But the role of conformation in crystallization is rather limited from a kinetic standpoint. If the dominant conformer (the global minimum) controls polymorphic selection, those polymorphs that employ the stable conformer as building unit would be selected. This is not the case: polymorph ON, which is composed of conformers that resemble the local minimum, is one of the fast-nucleating polymorphs from the melt.[43] This can be explained by the fact that the timescale for nucleation[44] is longer than the timescale for conformational changes in ROY. However, in situations where conformational changes are slow relative to crystal nucleation and growth, the distribution of conformers can potentially control polymorph selection.

Acknowledgements

We thank the National Science Foundation for supporting this work through the University of Wisconsin – Madison MRSEC (DMR-1720415).

References

[1] Yu, L.; Stephenson, G.; Mitchell, C.; Bunnell, C.; Snorek, S.; Bowyer, J.; Borchardt, T.; Stowell, J.; Byrn, S. Thermochemistry and Conformational Polymorphism of a Hexamorphic Crystal System. *J. Am. Chem. Soc.* **2000**, *122*, 585-591.

[2] Chen, S.; Guzei, I.; Yu, L. New Polymorphs of ROY and New Record for Coexisting Polymorphs of Solved Structures. *J. Am. Chem. Soc.* **2005**, *127*, 9881-9885.

[3] Yu, L. Polymorphism in Molecular Solids: An Extraordinary System of Red, Orange, And Yellow Crystals. *Acc. Chem. Res.* **2010**, *43*, 1257-1266.

[4] Tan, M.; Shtukenberg, A.; Zhu, S.; Xu, W.; Dooryhee, E.; Nichols, S.; Ward, M.; Kahr, B.; Zhu, Q. ROY Revisited, again: The Eighth Solved Structure. *Faraday Discuss.* **2018**, *211*, 477-491.

[5] Gushurst, K.; Nyman, J.; Boerrigter, S. The PO13 Crystal Structure Of ROY. *CrystEngComm* **2019**, *21*, 1363-1368.

[6] Tyler, A.; Ragbirsingh, R.; McMonagle, C.; Waddell, P.; Heaps, S.; Steed, J.; Thaw, P.; Hall, M.; Probert, M. Encapsulated Nanodroplet Crystallization of Organic-Soluble Small Molecules. *Chem* **2020**, *6*, 1755-1765.

[7] Lévesque, A.; Maris, T.; Wuest, J. ROY Reclaims Its Crown: New Ways to Increase Polymorphic Diversity. *J. Am. Chem. Soc.* **2020**, *142*, 11873-11883.

[8] Li, X.; Ou, X.; Rong, H.; Huang, S.; Nyman, J.; Yu, L.; Lu, M. The Twelfth Solved Structure of ROY: Single Crystals of Y04 Grown from Melt Microdroplets. *Cryst. Growth Des.* **2020**, *20*, 7093-7097.

[9] Vasileiadis, M.; Kazantsev, A. V.; Karamertzanis, P. G.; Adjiman, C. S.; Pantelides, C. C. The polymorphs of ROY: application of a systematic crystal structure prediction technique. *Acta Crystallogr., Sect. B: Struct. Sci.* **2012**, 68, 677−685.

[10] Nyman, J.; Yu, L.; Reutzel-Edens, S. Accuracy and Reproducibility in Crystal Structure Prediction: The Curious Case of ROY. *CrystEngComm* **2019**, *21*, 2080-2088.

[11] Greenwell, C.; McKinley, J.; Zhang, P.; Zeng, Q.; Sun, G.; Li, B.; Wen, S.; Beran, G. Overcoming the Difficulties of Predicting Conformational Polymorph Energetics in Molecular Crystals Via Correlated Wavefunction Methods. *Chem. Sci.* **2020**, *11*, 2200-2214.

[12] Greenwell, C.; Beran, G. Inaccurate Conformational Energies Still Hinder Crystal Structure Prediction in Flexible Organic Molecules. *Cryst. Growth Des.* **2020**, *20*, 4875-4881.

[13] Yu, L. Color Changes Caused by Conformational Polymorphism: Optical-Crystallography, Single-Crystal Spectroscopy, and Computational Chemistry. *J. Phys. Chem. A* **2002**, *106*, 544-550.

[14]Harty, E.; Ha, A.; Warren, M.; Thompson, A.; Allan, D.; Goodwin, A.; Funnell, N. Reversible Piezochromism in A Molecular Wine-Rack. *Chem. Commun.* **2015**, *51*, 10608-10611.

[15]Funnell, N.; Bull, C.; Ridley, C.; Capelli, S. Structural Behaviour Of OP-ROY at Extreme Conditions. *CrystEngComm* **2019**, *21*, 4473-4483.

[16] Tang, S.; Yusov, A.; Li, Y.; Tan, M.; Hao, Y.; Li, Z.; Chen, Y. S.; Hu, C. T.; Kahr, B.; Ward, M. D. ROY confined in hydrogen-bonded frameworks: coercing conformation of a chromophore. *Mater. Chem. Front*., **2020**, *4*, 2378-2383.

[17] Frisch, M. J.; Trucks, G. W.; Schlegel, H. B.; Scuseria, G. E.; Robb, M. A.; Cheeseman, J. R.; Scalmani, G.; Barone, V.; Petersson, G. A.; Nakatsuji, H., et al. *Gaussian 16*, Revision C.01; Gaussian, Inc.; Wallingford, CT, 2016.

[18] Jonsson, H.; Mills, G.; Jacobsen, K. In *Classical and Quantum Dynamics in Condensed Phase Simulations*; Berne, B., Ciccotti, G., Coker, D., Eds.; World Scientific: Singapore, 1998.

[19] Hjorth Larsen, A.; Jørgen Mortensen, J.; Blomqvist, J.; Castelli, I.; Christensen, R.; Dułak, M.; Friis, J.; Groves, M.; Hammer, B.; Hargus, C.; et al. The Atomic Simulation Environment—A Python Library for Working with Atoms. *J. Phys.: Condens. Matter* **2017**, *29*, 273002.

[20] McMahon, H.; Alfieri, K.; Clark, K.; Londergan, C. Cyanylated Cysteine: A Covalently Attached Vibrational Probe of Protein−Lipid Contacts. *J. Phys. Chem. Lett.* **2010**, *1*, 850-855.

[21] Waegele, M.; Culik, R.; Gai, F. Site-Specific Spectroscopic Reporters of The Local Electric Field, Hydration, Structure, And Dynamics of Biomolecules. *J. Phys. Chem. Lett.* **2011**, *2*, 2598-2609.

[22] Huang, C.; Wang, T.; Gai, F. Temperature Dependence of The CN Stretching Vibration of a Nitrile-Derivatized Phenylalanine in Water. *Chem. Phys. Lett.* **2003**, *371*, 731-738.

[23] Bagchi, S.; Fried, S. D.; Boxer, S. G. A Solvatochromic Model Calibrates Nitriles' Vibrational Frequencies to Electrostatic Fields. *J. Am. Chem. Soc.* **2012**, *134*, 10373−10376

[24] Renati, P.; Kovacs, Z.; De Ninno, A.; Tsenkova, R. Temperature Dependence Analysis of The NIR Spectra of Liquid Water Confirms The Existence of Two Phases, One of Which Is in A Coherent State. *J. Mol. Liq.* **2019**, *292*, 111449.

[25] Sillrén, P.; Matic, A.; Karlsson, M.; Koza, M.; Maccarini, M.; Fouquet, P.; Götz, M.; Bauer, T.; Gulich, R.; Lunkenheimer, P.; Loidl, A.; Mattsson, J.; Gainaru, C.; Vynokur, E.; Schildmann, S.; Bauer, S.; Böhmer, R. Liquid 1-Propanol Studied by Neutron Scattering, Near-Infrared, And Dielectric Spectroscopy. *J. Chem. Phys.* **2014**, *140*, 124501.

[26] Sun, Y.; Xi, H.; Ediger, M. D.; Richert, R.; Yu, L. Diffusion-Controlled and "Diffusionless" Crystal Growth near the Glass Transition Temperature: Relation between Liquid Dynamics and Growth Kinetics of Seven ROY Polymorphs. *J. Chem. Phys.* **2009**, *131*, 074506/1-074506/9.

[27] Li, T.; Ayers, P.; Liu, S.; Swadley, M.; Aubrey-Medendorp, C. Crystallization Force-A Density Functional Theory Concept for Revealing Intermolecular Interactions and Molecular Packing in Organic Crystals. *Chem. - Eu. J.* **2009**, *15*, 361-371.
[28] Cruz-Cabeza, A.; Bernstein, J. Conformational Polymorphism. *Chem. Rev.* **2013**, *114*, 2170-2191.
[29] Thomas, S.; Spackman, M. The Polymorphs Of ROY: A Computational Study of Lattice Energies and Conformational Energy Differences. *Aust. J. Chem.* **2018**, *71*, 279.
[30] Vasileiadis, M.; Kazantsev, A. V.; Karamertzanis, P. G.; Adjiman, C. S.; Pantelides, C. C. The polymorphs of ROY: application of a systematic crystal structure predition technique. *Acta Cryst.* **2012**, *B68*, 677-685.
[31] Li, H.; Stowell, J. G.; Borchardt, T. B.; Byrn, S. R. Synthesis, Conformational Polymorphism, and Construction of a G-T Diagram of 2-[(2-Nitrophenyl)amino]-3-thiophenecarbonitrile. *Cryst. Growth Des.* **2006**, *6*, 2469-2474.
[32] Cioslowski, J.; Scott, A.; Radom, L. Catastrophes, Bifurcations and Hysteretic Loops in Torsional Potentials of Internal Rotations in Molecules. *Mol. Phys.* **1997**, *91*, 413-420.
[33] Sugden, I.; Adjiman, C.; Pantelides, C. Accurate and Efficient Representation of Intramolecular Energy in ab Initio generation of Crystal Structures. I. Adaptive Local Approximate Models. *Acta Crystallogr., Sect. B: Struct. Sci., Cryst. Eng. Mater.* **2016**, *72*, 864-874.
[34] Palmer, A. NMR Characterization of The Dynamics of Biomacromolecules. *Chem. Rev.* **2004**, *104*, 3623-3640.
[35] Grevels, F.; Jacke, J.; Klotzbücher, W.; Krüger, C.; Seevogel, K.; Tsay, Y. Dynamic Processes On The IR Time Scale: Coalescence Of CO Stretching Vibrational Bands In[(H4-Diene)Fe(CO)3] Complexes. *Angew. Chem., Int. Ed. Engl.* **1987**, *26*, 885-887.
[36] Kim, Y.; Hochstrasser, R. Comparison of Linear and 2D IR Spectra in The Presence of Fast Exchange. *J. Phys. Chem. B* **2006**, *110*, 8531-8534.
[37] Xiao, J.; Gong, X.; Chiu, Y.; Xiao, H. Ab Initio Studies on The Conformations, Thermodynamic Properties and Rotational Isomerization of Diphenylamine (DPA). *J. Mol. Struct.: THEOCHEM* **1999**, *489*, 151-157.
[38] Poliak, P.; Vagánek, A. Torsional Deformation Effect on the N—H Bond Dissociation Energy in Diphenylamine. *Acta Chim. Slovaca* **2013**, *6*, 182-186.
[39] Lunazzi, L.; Magagnoli, C.; Guerra, M.; Macciantelli, D. Conformational Studies by Dynamic NMR. Part XV. The Rotational Barrier Of N-Methyl Aniline. *Tetrahedron Lett.* **1979**, *20*, 3031-3032.
[40] Lunazzi, L.; Magagnoli, C.; Macciantelli, D. Conformational Studies by Dynamic Nuclear Magnetic Resonance Spectroscopy. Part 19. Substituent Effects Upon the Rotational Barrier of Alkylanilines. *J. Chem. Soc., Perkin Trans. 2* **1980**, *11*, 1704.
[41] Davey, R.; Blagden, N.; Potts, G.; Docherty, R. Polymorphism in Molecular Crystals: Stabilization of A Metastable Form by Conformational Mimicry. *J. Am. Chem. Soc.* **1997**, *119*, 1767-1772.
[42] Blagden, N.; Davey, R. Polymorph Selection: Challenges for The Future? *Cryst. Growth Des.* **2003**, *3*, 873-885.
[43] Chen, S.; Xi, H.; Yu, L. Cross Nucleation between ROY Polymorphs. *J. Am. Chem. Soc.* **2005**, *127*, 17439-17444.

[44] Huang, C.; Chen, Z.; Gui, Y.; Shi, C.; Zhang, G.; Yu, L. Crystal Nucleation Rates in Glass-Forming Molecular Liquids: D-Sorbitol, D-Arabitol, D-Xylitol, And Glycerol. *J. Chem. Phys.* **2018**, *149*, 054503.

TOC Graphic